IL-18 neutralization ameliorates obstruction-induced epithelial–mesenchymal transition and renal fibrosis

Ahmad H. Bani-Hani[1], Jeffery A. Leslie[1], Hiroshi Asanuma[1], Charles A. Dinarello[2], Matthew T. Campbell[1], Daniel R. Meldrum[3], Honji Zhang[1], Karen Hile[1] and Kirstan K. Meldrum[1]

[1]Department of Urology, Indiana University School of Medicine, Indianapolis, Indiana, USA; [2]Department of Medicine, University of Colorado Health Sciences Center, Denver, Colorado, USA and [3]Department of Surgery, Indiana University School of Medicine, Indianapolis, Indiana, USA

Ureteral obstruction results in renal fibrosis in part due to inflammatory injury. The role of interleukin-18 (IL-18), an important mediator of inflammation, in the genesis of renal fibrosis was studied using transgenic mice overexpressing human IL-18-binding protein. In addition, HK-2 cells were analyzed following direct exposure to IL-18 compared to control media. Two weeks after ureteral obstruction, the kidneys of wild-type mice had a significant increase in IL-18 production, collagen deposition, α-smooth muscle actin and RhoA expression, fibroblast and macrophage accumulation, chemokine expression, and transforming growth factor-β1 (TGF-β1) and tumor necrosis factor-α (TNF-α) production, whereas E-cadherin expression was simultaneously decreased. The transgenic mice with neutralized IL-18 activity exhibited significant reductions in these indicators of obstruction-induced renal fibrosis and epithelial–mesenchymal transition, without demonstrating alterations in TGF-β1 or TNF-α activity. Similarly, the HK-2 cells exhibited increased α-smooth muscle actin expression and collagen production, and decreased E-cadherin expression in response to IL-18 stimulation without alterations in TNF-α or TGF-β1 activity. Our study demonstrates that IL-18 is a significant mediator of obstruction-induced renal fibrosis and epithelial–mesenchymal transition independent of downstream TGF-β1 or TNF-α production.

Kidney International (2009) **76,** 500–511; doi:10.1038/ki.2009.216; published online 17 June 2009

KEYWORDS: EMT; IL-18; TGF-β1; TNF-α; tubulointerstitial fibrosis

Correspondence: *Kirstan K. Meldrum, Riley Hospital for Children, 702 Barnhill Drive, Suite 4230, Indianapolis, Indiana 46202, USA. E-mail: kmeldrum@iupui.edu*

Received 27 August 2008; revised 14 April 2009; accepted 21 April 2009; published online 17 June 2009

Obstructive nephropathy is a major cause of renal dysfunction[1] characterized by progressive tubulointerstitial fibrosis.[2] Interstitial fibrosis is a complex pathophysiological process involving inflammatory cell infiltration, fibroblast proliferation, and an imbalance in extracellular matrix (ECM) synthesis, deposition, and degradation.[3–5] In the kidney, interstitial fibrosis is characterized by *de novo* activation of α-smooth muscle actin (SMA)-positive myofibroblasts, the principal effector cells responsible for excess ECM deposition. Growing evidence suggests that renal tubular epithelial cells (TECs) are capable of undergoing a phenotypic transformation into matrix-producing fibroblasts in pathologic states.[6–9] This transformation in the phenotype of the cell epithelial—mesenchymal transition (EMT) is thought to contribute greatly to renal fibrosis, with a large proportion of interstitial fibroblasts originating from TECs.[10,11] Epithelial cells that have undergone EMT are characterized by the loss of epithelial cell markers, such as E-cadherin, and *de novo* α-SMA expression.[12] The transformed epithelial cells also begin to express fibroblast (FSP-1), a marker specific for EMT.[13] TGF-β1 can independently initiate and complete the entire course of EMT, suggesting that induction of EMT may be a major pathway by which TGF-β1 stimulates interstitial fibrosis.[14–19] EMT appears to be integral to progressive TIF in diseased kidneys,[8,9,20] as selective blockade of EMT in animal models significantly reduces obstruction-induced fibrosis.[21,22]

IL-18 is a pro-inflammatory cytokine implicated in the pathogenesis of many inflammatory renal diseases, including renal ischemia–reperfusion injury, allograft rejection, and autoimmune disease.[23–28] In humans, IL-18 is a sensitive and early marker of renal tubular damage [26,29] and in animal models of renal ischemia–reperfusion injury, IL-18 exacerbates acute tubular necrosis.[30–32] A recent study suggests that IL-18 can also directly stimulate fibrotic changes in renal TECs *in vitro*,[33] and we therefore hypothesized that IL-18 is an important mediator of obstruction-induced renal fibrosis and EMT. To study this we examined renal cortical IL-18 production, collagen expression and deposition, α-SMA and RhoA expression, E-cadherin expression, FSP-1 and macrophage accumulation, chemokine expression, and TGF-β1 and

TNF-α production in male C57B16 wild type (WT) mice and mice transgenic for IL-18BP using a well-established model of unilateral urethral obstruction (UUO). C57BL6 mice transgenic for IL-18-binding protein transgenic (IL-18BP Tg) have been previously demonstrated to overexpress human IL-18-binding protein isoform *a* and reliably inhibit IL-18 activity.[34] In addition, human proximal tubular cells (HK-2) were directly stimulated with IL-18 and the cells were subsequently examined for α-SMA and E-cadherin expression, collagen production, and TGF-β1 and TNF-α activity.

RESULTS

IL-18 and IL-18BP production

Before surgical intervention, serum levels of human IL-18BP were measured and found to be dramatically elevated in the IL-18BP Tg mice when compared with WT mice (Figure 1a). Renal cortical tissue obtained from sham-operated animals revealed low levels of IL-18 production; however, IL-18 levels increased significantly in response to 1 or 2 weeks of obstruction (Figure 1b). IL-18 gene expression was similarly found to be significantly increased in WT animals exposed to 1 or 2 weeks of obstruction when compared with sham-treated animals (Figure 1c), whereas no significant change in IL-18 gene expression was detected in IL-18BP Tg animals exposed to the same degree obstruction.

Renal tissue sections were subsequently stained for IL-18. Minimal IL-18 was detected in sham-treated animals; however, a significant increase in renal cortical IL-18 staining was evident following 1 or 2 weeks of UUO (Figure 1d). IL-18 production predominantly localized to renal TECs, with minimal staining occurring in the glomeruli and interstitium.

Collagen expression and deposition

Renal tissue cross sections were analyzed for collagen I and III mRNA production and total soluble collagen concentration. Low levels of collagen I and III mRNA were present in sham-treated samples; however, collagen I and III mRNA expression significantly increased in WT mice exposed to 1 or 2 weeks of UUO (Figure 2a and b). In the obstructed IL-18BP Tg animals, collagen I and III mRNA levels were increased over sham levels, but significantly reduced when compared with WT-obstructed mice. Similarly, total renal collagen concentrations were significantly elevated in WT mice exposed to 1 or 2 weeks of UUO (Figure 2c). Although collagen concentrations were increased over sham levels in

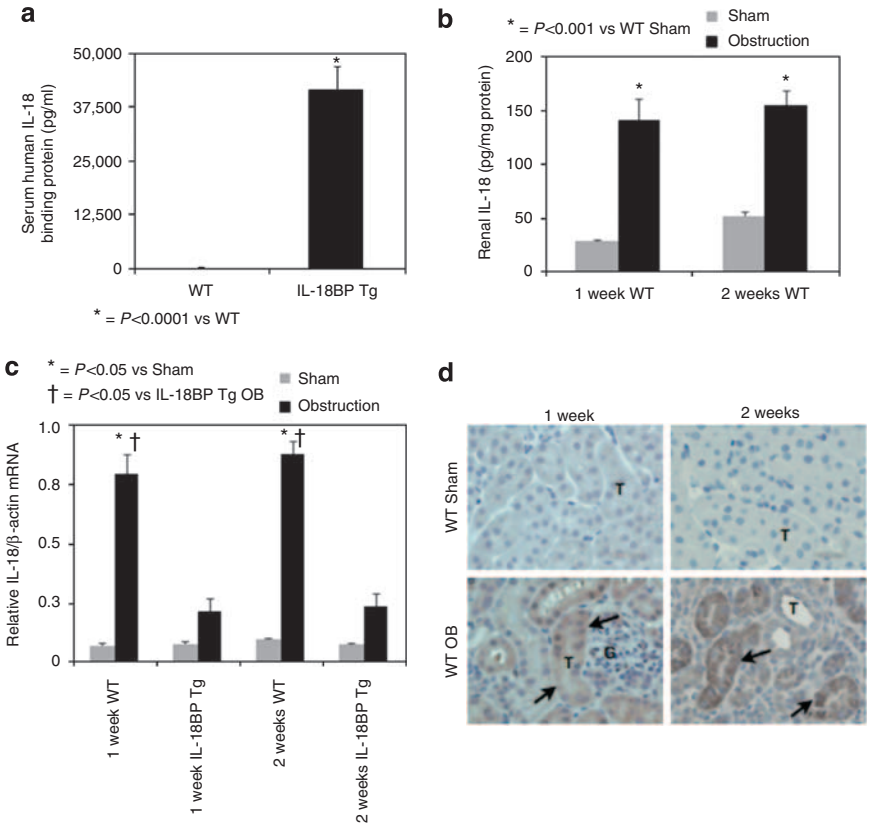

Figure 1 | Serum human IL-18BP levels and renal IL-18 production, quantitative mRNA expression, and immunolocalization following UUO. (**a**) Serum human IL-18BP levels (pg/ml) in WT or IL-18BP transgenic (IL-18BP Tg) animals. (**b**) Renal cortical IL-18 protein levels in WT sham and 1 or 2 week obstructed kidneys. (**c**) Quantitative IL-18 mRNA expression represented as a percentage of β-actin in WT and IL-18BP Tg animals exposed to sham operation or 1 or 2 weeks of UUO. (**d**) Renal cortical immunolocalization of IL-18 production (brown stain; arrows) in WT sham and 1- or 2-week obstructed kidneys (WT OB). G = glomerulus; T = tubule; OB, obstruction; UUO, unilateral urethral obstruction; WT, wild type. Original magnification ×400.

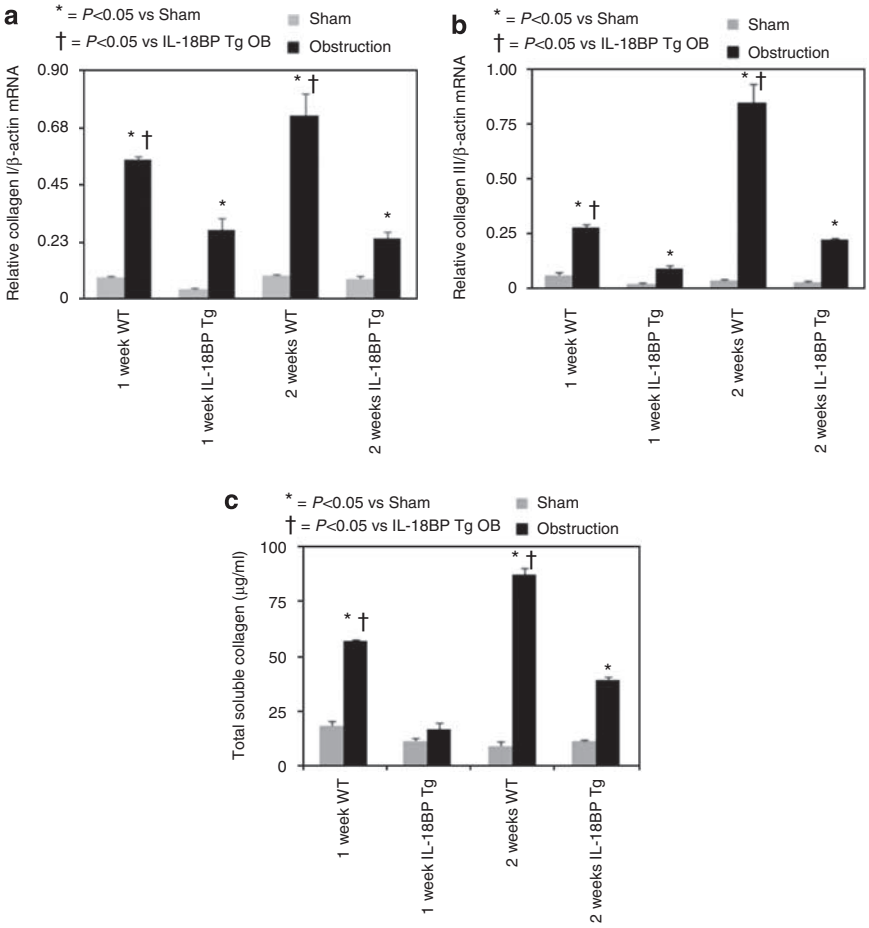

Figure 2 | Renal collagen I and III mRNA expression and total collagen concentration following UUO. (**a**) Quantitative collagen I mRNA expression represented as a percentage of β-actin in WT and IL-18BP transgenic (IL-18BP Tg) animals exposed to sham operation or 1 or 2 weeks of UUO. (**b**) Quantitative collagen III mRNA expression represented as a percentage of β-actin in WT and IL-18BP Tg animals exposed to sham operation or 1 or 2 weeks of UUO. (**c**) Total soluble collagen concentration in renal tissue sections obtained from WT and IL-18BP Tg animals exposed to sham operation or 1 or 2 weeks of UUO.

the 2-week obstructed IL-18BP Tg mice, collagen levels were significantly reduced in both groups of obstructed IL-18BP Tg animals when compared with obstructed WT mice. This suggests that IL-18 neutralization protects against obstruction-induced collagen gene expression and collagen deposition.

Masson's trichrome and α-SMA staining corroborated the collagen findings. Although sham-operated animals exhibited little collagen deposition and α-SMA staining (localizing only to the vascular wall) in renal tissue sections, a significant increase in both collagen and α-SMA deposition was evident in the WT-obstructed kidneys (Figure 3a and b), and the degree of collagen and α-SMA deposition was considerably greater in the WT kidneys exposed to 2 weeks of UUO. The 1-week WT obstruction group showed moderate α-SMA and trichrome staining (2+), whereas the 2-week WT obstruction group showed moderate to severe α-SMA and trichrome staining (2 to 3+), each being more prominent in the medulla. In contrast, the IL-18BP Tg samples exposed to the same degree of obstruction exhibited mild (1+) α-SMA and trichrome staining that was significantly less prominent than that observed in the WT-obstructed samples.

α-SMA, E-cadherin, and RhoA expression

To assess IL-18's role in obstruction-induced EMT, renal cortical tissue was subjected to western blot analysis for α-SMA and E-cadherin. A significant increase in α-SMA expression was detected in WT mice subjected to 1 or 2 weeks of UUO when compared with sham-operated animals (Figure 4a and d). IL-18BP Tg mice subjected to the same degree of obstruction; however, demonstrated no significant increase in α-SMA expression. A marked reduction in E-cadherin expression was simultaneously detected in WT mice subjected to one or two weeks of UUO (Figure 4b); however, no significant reduction in E-cadherin expression was detected in obstructed IL-18BP Tg mice exposed to the same degree of obstruction. These findings suggest that IL-18 neutralization prevents the early stages of obstruction-induced EMT.

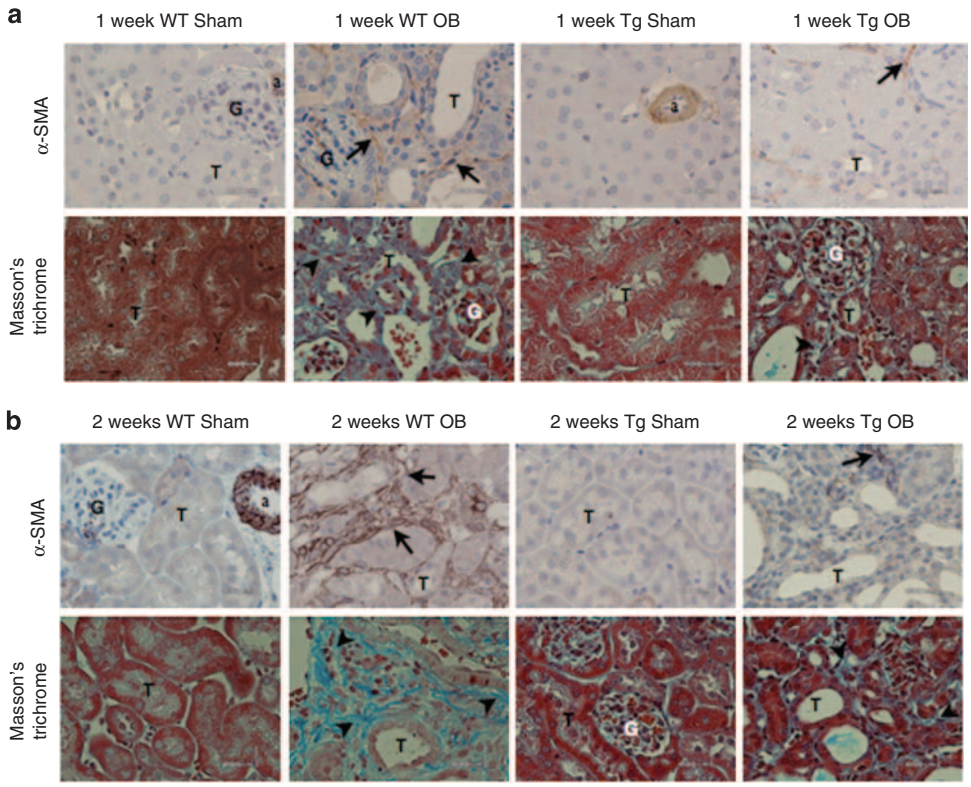

Figure 3 | Renal cortical α-SMA deposition and Masson's trichrome staining following UUO. Photographs (original magnification ×400) depicting renal cortical α-SMA deposition (brown stain; arrows) and collagen deposition (blue stain; arrowheads) in WT and IL-18BP transgenic animals exposed to sham operation (WT Sham; Tg Sham) or 1 or 2 weeks of UUO (WT OB; Tg OB). a = arteriole; G = glomerulus; T = tubule. (**a**) One-week samples. (**b**) Two-week samples.

Ras homolog gene family member A (RhoA) as mediator of α-SMA promotor activation and EMT, was subsequently evaluated in renal cortical tissue sections. A significant increase in RhoA expression was detected in WT mice subjected to 1 or 2 weeks of UUO when compared with sham-operated animals (Figure 4c). However, IL-18BP Tg mice subjected to the same degree of obstruction demonstrated no increase in RhoA expression, suggesting that IL-18-induced EMT may be mediated, in part, through alterations in RhoA.

Fibroblast accumulation

IL-18-induced renal tubular cell EMT was further evaluated by counting the number of FSP-1+ cells in renal cortical tissue sections. Although the number of FSP-1+ cells increased significantly in WT mice subjected to renal obstruction (Figure 5a–c), and was most pronounced in WT mice subjected to 2 weeks of renal obstruction, a marked reduction in FSP-1+ cells was detected in both groups of obstructed IL-18BP Tg mice when compared with WT mice. These findings provide further evidence that IL-18 neutralization prevents EMT and fibroblast accumulation within the interstitium.

Macrophage infiltration

Renal cortical tissue sections were stained with a rat anti-mouse macrophage antibody to assess the degree of macrophage infiltration during renal obstruction. Although sham-treated samples exhibited minimal macrophage staining (Figure 5a, b and d), WT mice subjected to 1 or 2 weeks of renal obstruction demonstrated significant interstitial macrophage accumulation. This was most pronounced in response to 2 weeks of UUO. The degree of macrophage accumulation, although significantly increased over sham levels, was reduced in both groups of obstructed IL-18BP Tg mice when compared with WT mice.

Chemokine expression

Renal cortical tissue sections were analyzed for chemokine ligand 3 (CCL3) and chemokine ligand 4 (CCL4) mRNA expression. A significant increase in both CCL3 and CCL4 gene expression was detected in WT mice subjected to 1 or 2 weeks of UUO (Figure 6a and b), and was most pronounced after 2 weeks of UUO. IL-18BP Tg mice subjected to the same degree of obstruction; however, demonstrated no increase in CCL3 or CCL4 gene expression, suggesting that IL-18 contributes to obstruction-induced renal inflammation, in part, through alterations in chemokine expression.

TGF-β1 production

Renal cortical tissue obtained from sham-operated animals revealed minimal TGF-β1 mRNA expression (Figure 7a). Relative TGF-β1 mRNA levels increased significantly in response to 1 or 2 weeks of renal obstruction in both WT

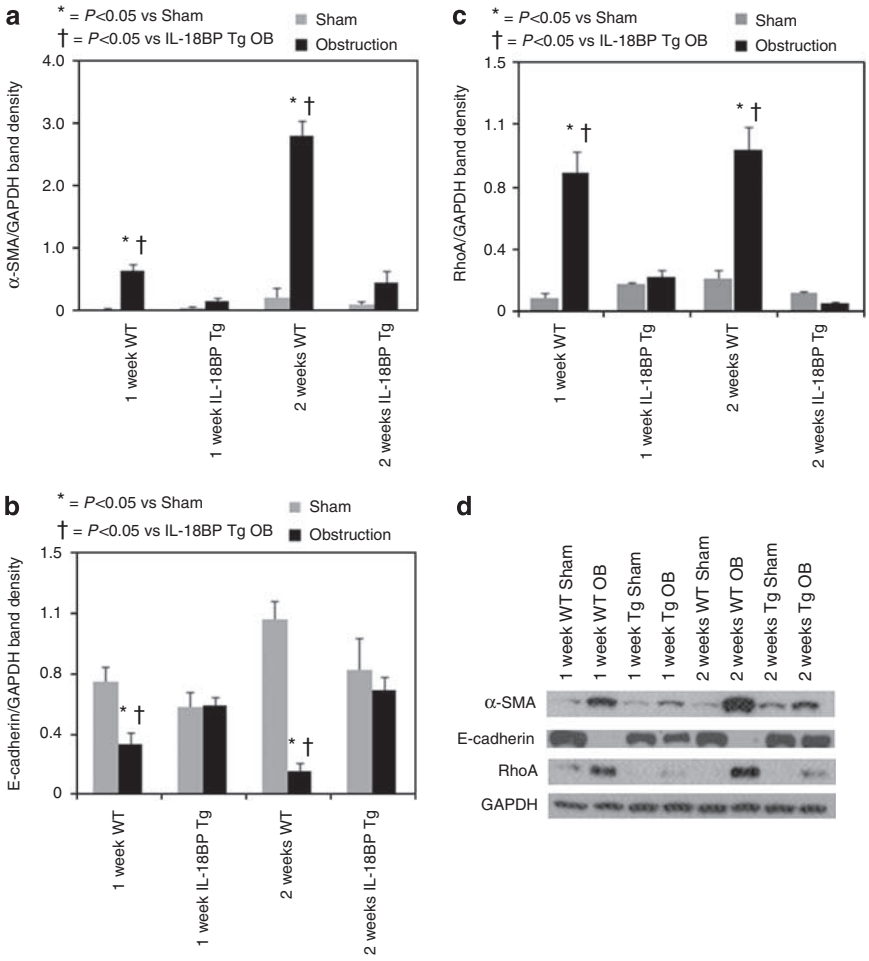

Figure 4 | Renal cortical E-cadherin, α-SMA, and RhoA expression following UUO. (**a**) Densitometric analysis of α-SMA expression represented as a percentage of GAPDH in WT and IL-18BP transgenic (IL-18BP Tg) animals exposed to sham operation or 1 or 2 weeks of UUO. (**b**) Densitometric analysis of E-cadherin expression represented as a percentage of GAPDH. (**c**) Densitometric analysis of RhoA expression represented as a percentage of GAPDH. (**d**) Gel photograph depicting E-cadherin, α-SMA, RhoA, and GAPDH expression in WT and IL-18BP transgenic animals exposed to sham operation (WT Sham; Tg Sham) or 1 or 2 weeks of UUO (WT OB; Tg OB).

and IL-18BP Tg animals; however, no difference in TGF-β1 mRNA expression was observed between WT or IL-18BP Tg animals exposed to the same degree of obstruction.

Renal cortical active TGF-β1 protein levels were similarly elevated in response to ureteral obstruction, as shown in Figure 7b. Although sham-operated animals demonstrated low levels of TGF-β1, renal cortical TGF-β1 levels increased significantly in response to 1 or 2 weeks of obstruction in both WT and IL-18BP Tg animals. Again, no difference in active TGF-β1 levels were observed between WT and IL-18BP Tg animals exposed to the same degree of obstruction.

TNF-α production

Renal cortical tissue obtained from sham-operated animals revealed minimal TNF-α mRNA expression (Figure 8a). Relative TNF-α mRNA levels increased significantly in response to 1 or 2 weeks of renal obstruction in both WT and IL-18BP Tg animals; however, no difference in TNF-α mRNA expression was observed between WT and IL-18BP Tg animals exposed to the same degree of obstruction.

Renal cortical TNF-α levels were similarly elevated in response to ureteral obstruction, as shown in Figure 8b. Although sham-operated animals demonstrated low levels of TNF-α, renal cortical TNF-α levels increased significantly in response to 1 or 2 weeks of obstruction in both WT and IL-18BP Tg animals, and again, no difference in TNF-α levels were observed between WT and IL-18BP Tg animals exposed to UUO. These results suggest that IL-18's downstream pro-fibrotic effects occur independent of TGF-β1 and TNF-α activity.

α-SMA and E-cadherin expression *in vitro*

To further elucidate IL-18's role in EMT, HK-2 cells were directly stimulated with varying concentrations of IL-18 *in vitro* and examined. Cells exposed to increasing concentrations of IL-18 demonstrated a progressive increase in α-SMA and a progressive decrease in E-cadherin expression (Figure 9a and b), suggesting that IL-18 stimulates the transformation of HK-2 epithelial cells into myofibroblasts. These observations were confirmed with immunofluorescent staining for α-SMA, which

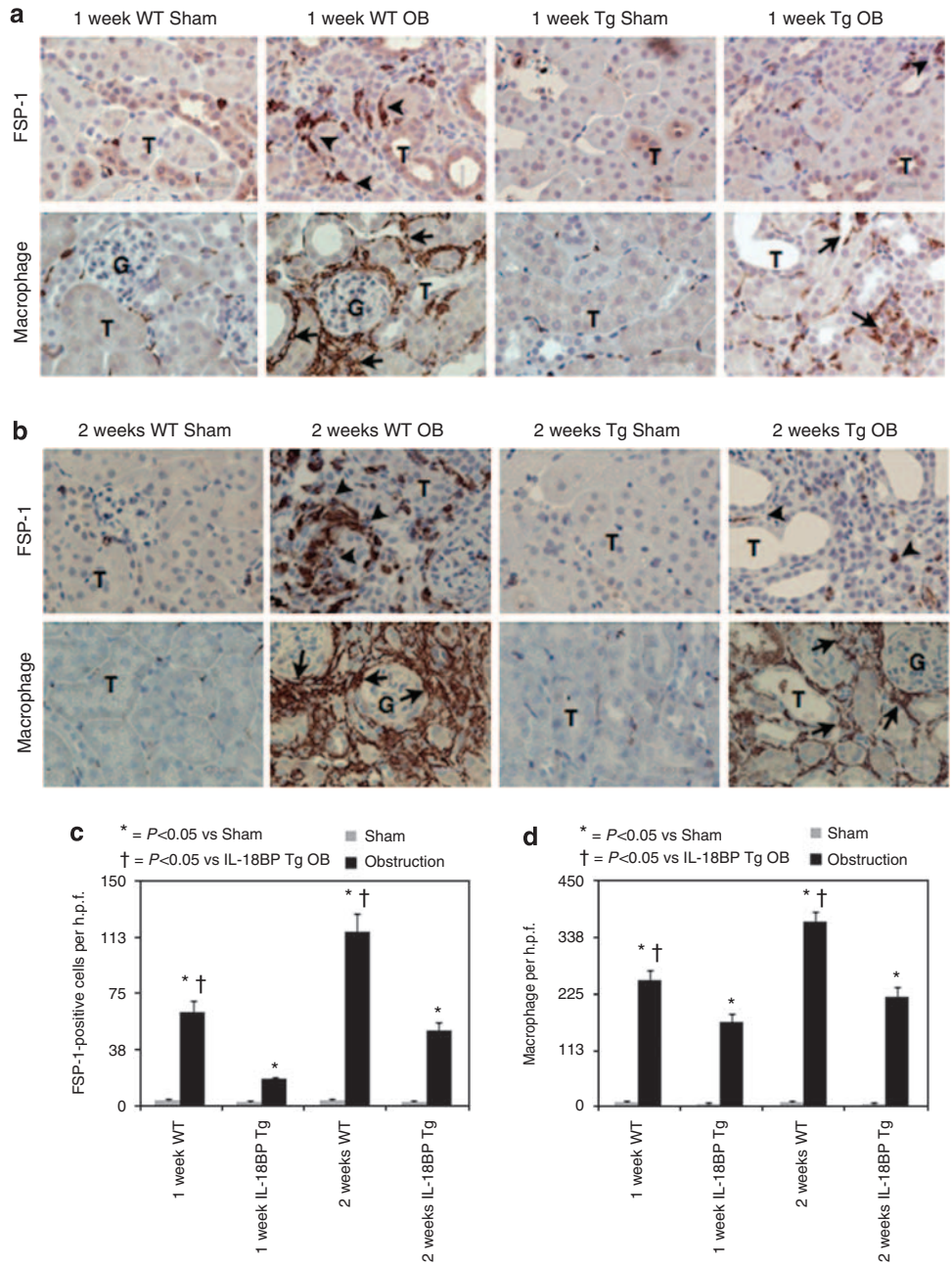

Figure 5 | Renal cortical FSP-1 + and macrophage accumulation following UUO. (**a**) Photographs (original magnification ×400) depicting FSP-1 + cells (brown stain; arrowheads) and macrophage (brown stain; arrows) in WT and IL-18BP transgenic animals exposed to sham operation (WT Sham; Tg Sham) or 1 or 2 weeks of UUO (WT OB; Tg OB). G = glomerulus; T = tubule. (**a**) One-week samples (**b**) Two-week samples. (**c**, **d**) Semiquantitative renal cortical FSP-1 + and macrophage accumulation following UUO. (**c**). Number of FSP-1 + cells/h.p.f. (**d**) Number of macrophages/h.p.f. h.p.f. = high-powered field.

revealed a significant increase in the number of α-SMA + cells in response to IL-18 stimulation (Figure 9c), and further, that the α-SMA + HK-2 cells had the morphological characteristics of myofibroblasts. These characteristics were not observed in HK-2 cells exposed to control media.

Total collagen, TNF-α, and TGF-β1 production *in vitro*

To investigate the secretory activity of HK-2 cells, supernatants were collected and assayed for total collagen, TNF-α, and TGF-β1 production following cell stimulation with varying concentrations of IL-18. Although total collagen production increased significantly in response to increasing concentrations of IL-18 (Figure 10a), no increase in either TNF-α or TGF-β1 production was observed at any concentration of IL-18 (Figure 10b).

DISCUSSION

Tubulointerstitial fibrosis is a major pathological component of obstructive renal injury.[35] The pathophysiology of tubulointerstitial fibrosis involves fibroblast proliferation,

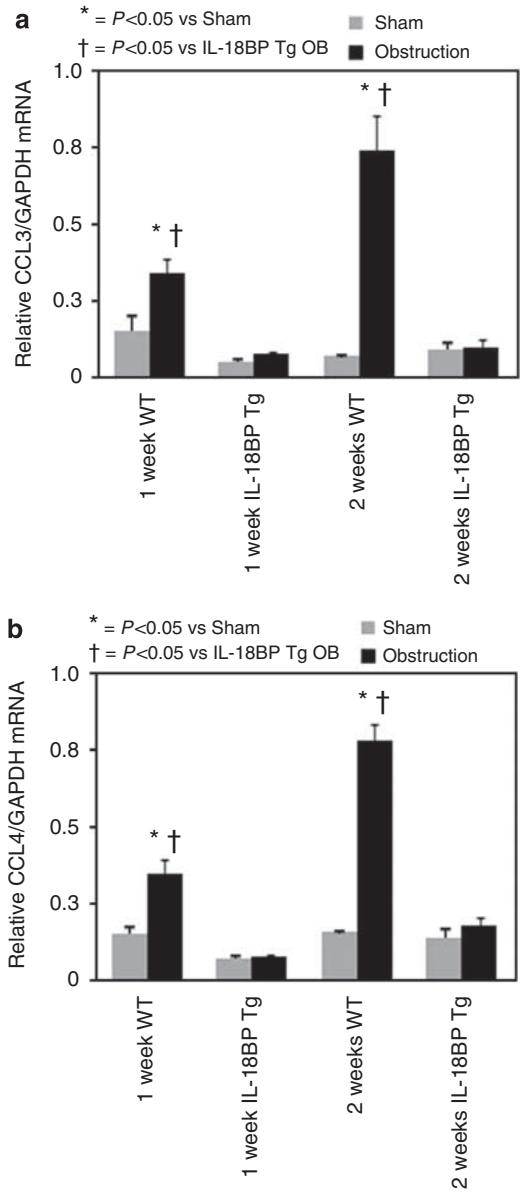

Figure 6 | Quantitative renal cortical CCL3 and CCL4 mRNA expression following UUO. (**a**) Quantitative CCL3 mRNA expression represented as a percentage of GAPDH in WT and IL-18BP transgenic (IL-18BP Tg) animals exposed to sham operation or 1 or 2 weeks of UUO. (**b**) Quantitative CCL4 mRNA expression represented as a percentage of GAPDH in WT and IL-18BP Tg animals exposed to sham operation or 1 or 2 weeks of UUO.

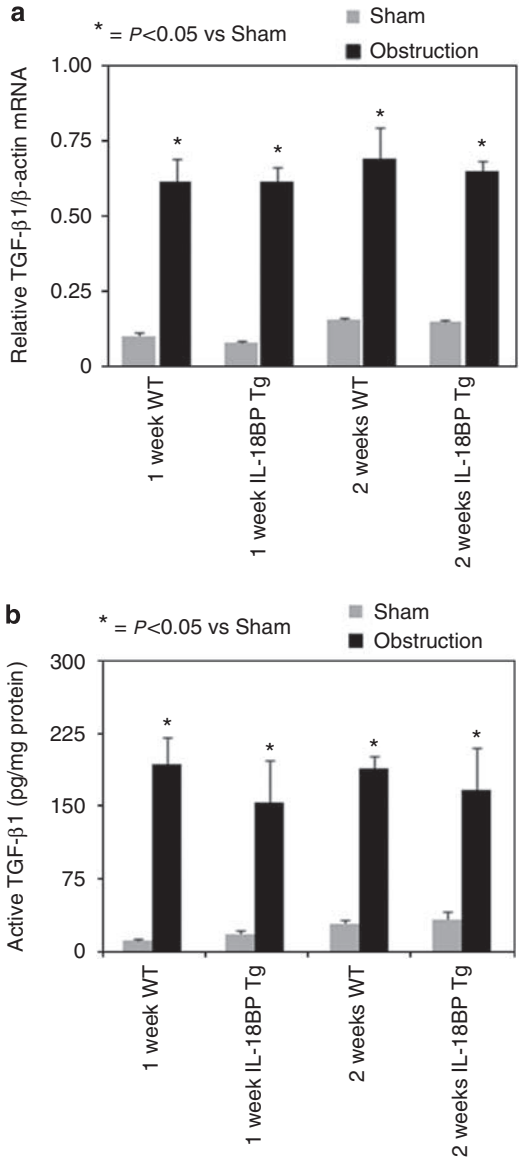

Figure 7 | Quantitative renal cortical TGF-β1 mRNA expression and protein production following UUO. (**a**) Quantitative TGF-β1 mRNA expression represented as a percentage of β-actin in WT and IL-18BP transgenic (IL-18BP Tg) animals exposed to sham operation or 1 or 2 weeks of UUO. (**b**) Active TGF-β1 protein levels in WT and IL-18BP Tg animals exposed to sham operation or 1 or 2 weeks of UUO.

macrophage infiltration, the elaboration of cytokines, and an imbalance in ECM deposition and degradation. Fibroblasts are recognized as the principle effector cells responsible for ECM deposition under pathologic conditions, and accumulating evidence suggests that a large proportion of collagen-producing interstitial fibroblasts originate from TECs.[9,11,16] Indeed, EMT appears to be integral to renal fibrogenesis, as selective blockade of EMT can dramatically reduce well-established tubulointerstitial fibrosis.[19,22] TGF-β1 is a major regulator of fibrosis through stimulation of EMT and fibroblast proliferation,[12,19,21,36–39] extracellular matrix synthesis,[3,39–43] and the simultaneous inhibition of collagenase and degradative matrix metalloproteinases.[3,39,41,44] Although increased TGF-β1 production has long been regarded as the final common pathway in renal fibrogenesis, this is the first study to demonstrate that IL-18 is an important mediator of obstruction-induced renal fibrosis and EMT independent of downstream TGF-β1, and TNF-α production.

IL-18 is a recently discovered pro-inflammatory cytokine that is structurally and functionally related to the IL-1 family, and a potent stimulator of cytokine gene expression through

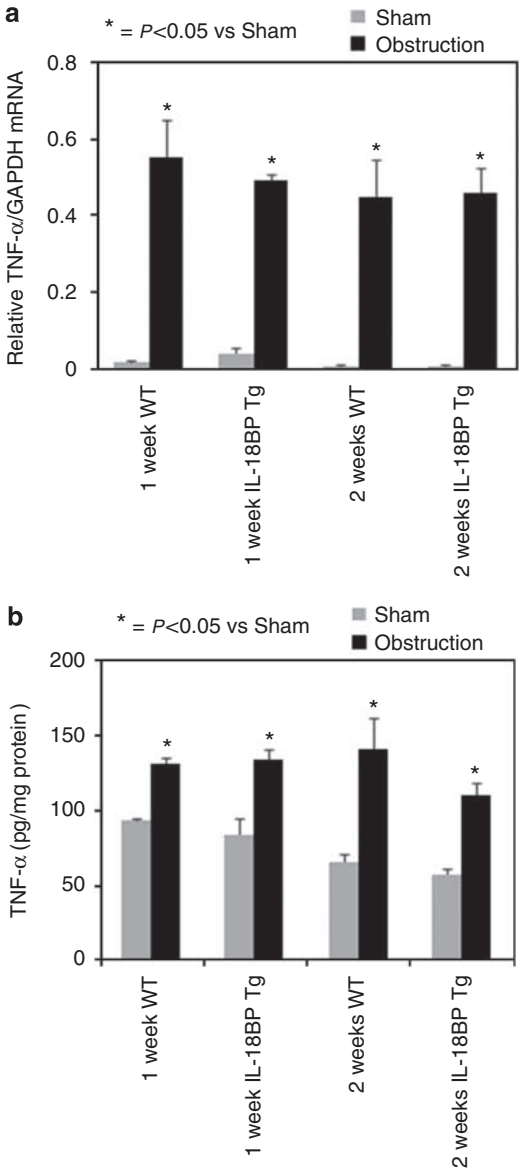

Figure 8 | Quantitative renal cortical TNF-α mRNA expression and protein production following UUO. (**a**) Quantitative TNF-α mRNA expression represented as a percentage of GAPDH in WT and IL-18BP transgenic (IL-18BP Tg) animals exposed to sham operation or 1 or 2 weeks of UUO. (**b**) TNF-α protein levels in WT and IL-18BP Tg animals exposed to sham operation or 1 or 2 weeks of UUO.

activation of NF-κB. In humans, urinary IL-18 levels are a sensitive and early marker of renal tubular damage from ischemic and post-transplantation ATN,[29] and in animal models, a significant decrease in ischemia-induced renal dysfunction and ATN has been observed in IL-18-deficient mice.[45,46] Our data reveals that renal cortical IL-18 production is three to five times higher, and IL-18 mRNA expression is eight times higher in obstructed kidneys when compared with sham-operated animals. This is supported by our observation that renal TECs show a significant increase in IL-18 staining in response to UUO. Other studies have documented a significant increase in circulating IL-18 levels and IL-18 receptor expression in patients with chronic kidney disease,[25,33,47] and have similarly localized IL-18 production to TECs in these patients.[33] In conjunction with our observations, these studies suggest that IL-18 may be an important mediator of renal fibrogenesis.

To evaluate IL-18's role in obstruction-induced tubulointerstitial fibrosis, renal samples were analyzed for collagen I and III gene expression, total collagen content, collagen and α-SMA deposition, and evidence of EMT, in WT and IL-18BP Tg mice. In addition, human proximal tubular cells (HK-2) were directly stimulated with IL-18 and the cells subsequently examined for α-SMA expression, collagen production, and EMT. Our results demonstrate a significant reduction in obstruction-induced collagen I and III mRNA expression and total collagen concentration in mice transgenic for IL-18BP. Furthermore, renal tissue staining revealed a marked reduction in obstruction-induced collagen deposition (Masson's trichrome) and α-SMA accumulation in IL-18BP Tg animals. These observations are supported by our *in vitro* studies in which direct cell stimulation with IL-18 induced α-SMA expression and collagen production in a concentration-dependent fashion, and by other recent studies demonstrating that direct cell stimulation with IL-18 induces collagen I, α-SMA, and fibronectin production in a dosage and time-dependent fashion.[33]

Epithelial–mesenchymal transition was subsequently evaluated by examining the renal cortical expression of the epithelial cell marker, E-cadherin, the myofibroblast marker, α-SMA, and the fibroblast marker specific for EMT and FSP-1. Cell morphology, α-SMA, and E-cadherin expression were also examined following direct IL-18 stimulation of HK-2 cells *in vitro*. Renal obstruction resulted in a significant reduction in E-cadherin expression and a simultaneous increase in α-SMA expression, indicating a transition between epithelia and mesenchyme. This was confirmed with the observation that increased numbers of FSP-1+ fibroblasts were present in the interstitium of obstructed kidneys when compared with sham-treated controls. Overexpression of IL-18BP during renal obstruction dramatically inhibited this process, resulting in preservation of E-cadherin expression, a marked reduction in α-SMA expression, and a marked decrease in the number of FSP-1+ fibroblasts. Furthermore, direct stimulation of HK-2 cells with IL-18 *in vitro* resulted in a significant reduction in E-cadherin expression, a significant increase in α-SMA expression, an increase in the number of α-SMA+ cells, and the morphological conversion of α-SMA+ cells into cells characteristic of fibroblasts. IL-18 therefore appears to have potent pro-fibrotic properties and a direct role in the pathogenesis of obstruction-induced EMT.

To evaluate the mechanisms of IL-18's pro-fibrotic effect, we investigated macrophage infiltration and the expression and production of TGF-β1 and TNF-α during UUO in WT and IL-18BP Tg mice. Production of TGF-β1 and TNF-α was also evaluated following direct cell stimulation with IL-18

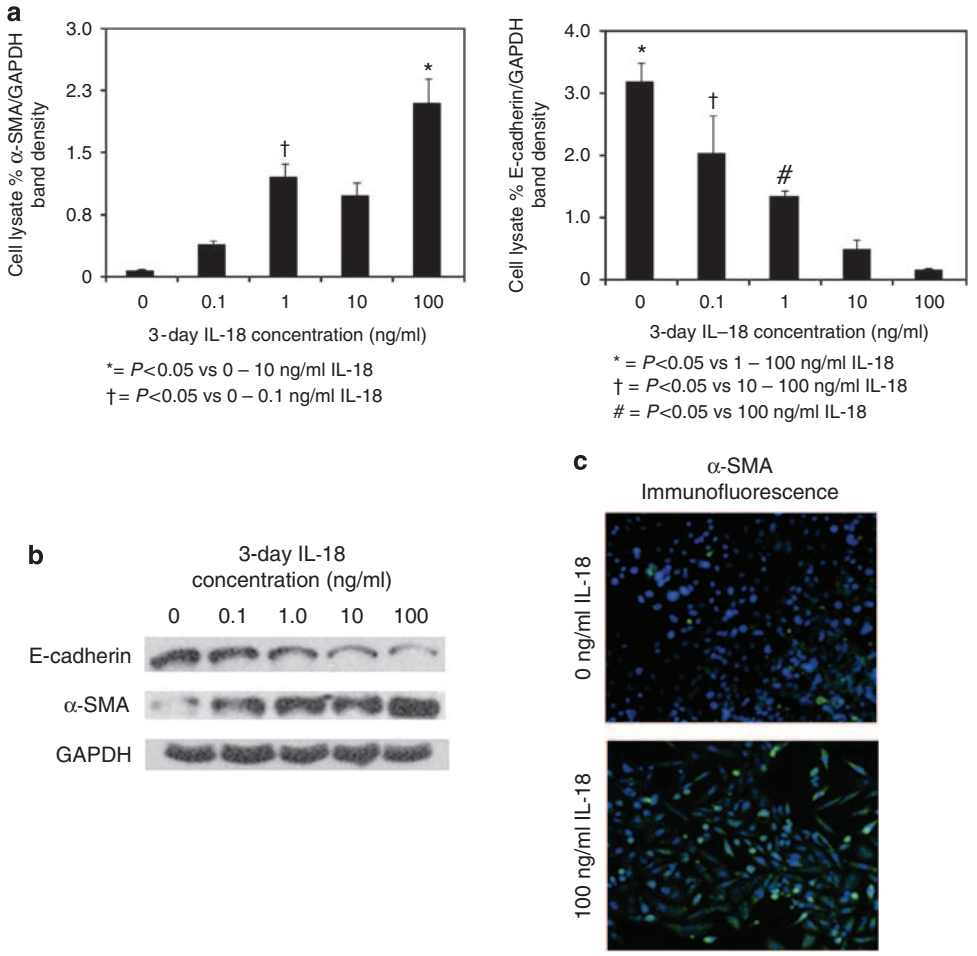

Figure 9 | HK-2 cell expression of α-SMA and E-cadherin following IL-18 stimulation *in vitro*. (**a**) Cell lysate α-SMA and E-cadherin expression represented as a percentage of GAPDH in response to 3 days of cell stimulation with varying concentrations of recombinant human IL-18 (0–100 ng/ml). (**b**) Corresponding gel photograph representing E-cadherin, α-SMA, and GAPDH bands at various IL-18 concentrations after 3 days of cell stimulation. (**c**) Photograph (original magnification ×400) of α-SMA immunofluorescent staining in untreated and IL-18-stimulated cells (100 ng/ml for 3 days). α-SMA staining is green and nuclei are stained blue.

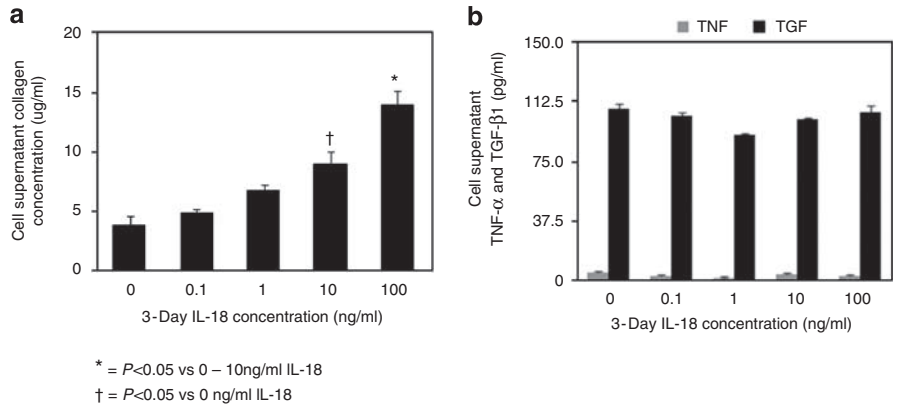

Figure 10 | HK-2 cell supernatant collagen, TGF-β1, and TNF-α levels following IL-18 stimulation *in vitro*. (**a**) Cell supernatant total collagen levels (μg/ml) in response to 3 days of cell stimulation with varying concentrations of recombinant human IL-18 (0–100 ng/ml). (**b**) Cell supernatant active TGF-β1 and TNF-α levels (pg/ml) in response to 3 days of cell stimulation with varying concentrations of IL-18 (0–100 ng/ml).

in vitro. It has been clearly established that TGF-β1 is a major regulator of renal fibrosis by the stimulation of fibroblast proliferation and extracellular matrix synthesis,[3,37–42,48] and TGF-β1 is independently capable of inducing and completing the entire EMT process *in vitro*.[12,15–19,21,36] TNF-α also has a role in fibrotic renal injury, stimulating ECM accumulation,

inhibition of ECM degradation, and the upregulation of a number of cytokines and transcription factors involved in tubulointerstitial fibrosis, including TGF-β1 and NF-κB.[49–53] Although we did observe an increase in renal TGF-β1 and TNF-α production in response to obstruction, no reduction in either TGF-β1 or TNF-α gene expression or protein levels were detected in the IL-18BP Tg animals, despite the rather dramatic decrease in obstruction-induced renal fibrosis in these animals. Furthermore, direct stimulation of HK-2 cells with IL-18 *in vitro* did not alter supernatant levels of either TGF-β1 or TNF-α at any concentration examined, even though the cells were undergoing molecular and morphologic changes consistent with EMT in response to IL-18. This finding suggests that IL-18 mediates its downstream pro-fibrotic effect independent of these two mediators. Although the mechanism of IL-18's pro-fibrotic effect remains unclear, our findings do reveal that IL-18 neutralization causes a reduction in obstruction-induced chemokine expression (CCL3 and CCL4), macrophage infiltration, and RhoA expression, an intracellular mediator of EMT.[54] IL-18 has also been shown to inhibit matrix metalloproteinase activity in chondrocytes.[55] It is therefore likely that IL-18 exerts its pro-fibrotic effect by impacting signaling mediators downstream of TGF-β1 and TNF-α, and by stimulating inflammatory cell infiltration during UUO. Collectively, this is the first demonstration that IL-18 neutralization ameliorates obstruction-induced EMT and tubulointerstitial fibrosis *in vivo*, and accordingly identifies IL-18 as an important mediator of obstruction-induced renal injury.

Obstructive renal injury stimulates a cascade of events that culminate in tubulointerstitial fibrosis and the conversion of normal TECs into matrix-producing fibroblasts. This study identifies IL-18 as an important mediator of obstruction-induced tubulointerstitial fibrosis and EMT, independent of downstream TGF-β1 and TNF-α activity. This represents a novel signaling pathway in the pathogenesis of renal fibrosis, and as the mechanism of IL-18's pro-fibrotic effect becomes more clearly defined, new therapeutic strategies aimed at ameliorating renal fibrosis may be realized.

MATERIALS AND METHODS

Animals, experimental groups, and operative techniques

The animal protocol was reviewed and accepted by the Indiana University Animal Care and Use Committee. Male C57BL6 mice transgenic for IL-18-binding protein (IL-18 BP Tg) were generously donated by Dr Charles Dinarello from the University of Colorado Health Science Center, Denver, Colorado. These mice overexpress human IL-18-binding protein isoform *a* and reliably inhibit IL-18 activity,[34] but do not have any notable phenotype. The genotype of the mice was confirmed with a PCR analysis of extracted DNA samples from tail snips (5′ primer, 5′-ACACCTGTCTCGCAGACC AC-3′ and 3′ primer, 5′-TCAGCTGCTCCAGCACCAA-3′) as described by Fantuzzi *et al*[34] and overexpression of serum levels of human IL-18BP was confirmed using an ELISA (Figure 1a), before utilization of the animals.

Male mice weighing 25–30 g (six animals per group) were anesthetized with isofluorane and the left ureter was isolated and completely ligated with 5–0 silk suture. Sham-operated mice underwent an identical surgical procedure without ureteral ligation. One or two weeks postoperatively, mice were re-anesthetized, the left kidneys removed and snap frozen in liquid nitrogen, and the animals subsequently killed.

Tissue homogenization

A portion of each renal cortex was homogenized after the samples had been diluted in 10 volumes of homogenate buffer per gram of tissue (10 mM Hepes (pH 7.9), 10 mM KCL, 0.1 mM EGTA, 1 mM DTT, and Complete Protease Inhibitor tabs (Boehringer Mannheim, Indianapolis, IN, USA)) using a vertishear tissue homogenizer. Renal homogenates were then centrifuged at 3000 *g* for 15 min, and the supernatants stored at −70 °C until the ELISA assays/western blots could be performed.

Cell culture and IL-18 stimulation

The human proximal tubular cell line HK-2 was cultured in keratinocyte serum-free medium + 5 ng/ml epidermal growth factor (EGF) and 40 mg/ml bovine extract + 100 U/ml penicillin and 100 Ug/ml of streptomycin. The cells were passaged weekly by trypsinization (0.25% trypsin, 0.02% EDTA) following formation of a confluent monolayer and placed in serum-free media 24 h before stimulation. Recombinant mature IL-18 (R&D Systems, Minneapolis, MN, USA) was added to the cells at concentrations of 0.1 ng/ml, 1 ng/ml, 10 ng/ml, or 100 ng/ml,[33] with untreated cells serving as controls. The cells were exposed to the single dose of IL-18 vs untreated media for 3 days and both supernatants and cell lysates were harvested (four plates per treatment group).

IL-18BP, IL-18, active TGF-β1, and TNF-α levels

Serum human IL-18BP levels, renal homogenate IL-18, active TGF-β1, TNF-α, and levels, and cell supernatant active TGF-β1, and TNF-α levels were determined using an ELISA (human IL-18BP: BD Biosciences, San Diego, CA, USA; mouse IL-18: MBL Int., Woburn, MA, USA; mouse and human TGF-β1: R&D Systems; mouse and human TNF-α: BD Biosciences). For active TGF-β1, latent TGF-β1 was activated by adding 1N HCL to each sample at 1:25 for 60 min at 4 °C. The samples were then neutralized with 1N NaOH and immediately tested. The ELISA was performed by adding 100 µl of each sample to wells in a 96-well plate of a commercially available ELISA kit and the assay performed according to the manufacturer's instructions. All samples were tested in duplicate. The ELISA results were expressed as pg/mg protein for tissue and pg/ml for serum/supernatant.

The renal cortical levels of IL-18 were not presented for the IL-18BP transgenic mice because levels were dramatically higher than WT animals in every treatment group examined, including the shams. This led us to believe that the extreme overproduction of IL-18BP in these animals may somehow interfere with the ELISA, rendering it inaccurate. We therefore relied on IL-18 mRNA production as a more accurate reflection of IL-18 production in the IL-18BP Tg animals.

Real-time PCR

Total RNA was extracted from the renal cortical tissue by homogenization in Trizol (Gibco BRL, Gaithersburg, MD, USA), then isolated by precipitation with chloroform and isopropanol as previously described.[56] Total RNA (0.5 µg) was subjected to cDNA synthesis using iScript (Bio-Rad, Hercules, CA, USA). cDNA from each sample was analyzed for IL-18 (Mm00434226_m1), Collagen 1a2

(Mm01165187_m1), Collagen 3a1 (Mm00802331_m1), CCL3 (Mm00441259_g1), CCL4 (Mm00443111_m1), TGF-β1 (Mm01178820_m1), and TNF-α (Mm00443258_m1) using a TaqMan gene expression assay (RT-PCR; Applied Biosystems, Foster City, CA, USA). FAM Dye/MGB-labeled probes for either mouse β-actin or GAPDH (Applied Biosystems) served as endogenous controls.

Tissue and cell supernatant total collagen concentration

The total soluble collagen concentration within renal cortical tissue sections and cell supernatants (four per group) were measured with the Sircol collagen assay kit (Accurate Chemical and Scientific, Westbury, NY) according to the manufacturer's protocol. Dry tissue samples were dissolved in 0.5 M acetic acid and heated for 120 min at 60 °C. Tissue suspensions were centrifuged, supernatants collected, and the total collagen concentration measured at 540 nm in all collected supernatants.

IL-18 and α-SMA tissue staining

Tissue sections (4 μm) were deparaffinized and dehydrated with alcohol. Sections were permeabilized, subjected to an Avidin/Biotin block (Avidin/Biotin Blocking kit; Vector labs, Burlingame, CA, USA) for 15 min, and non-specific binding sites were subsequently blocked with normal horse serum. Slides were incubated with a goat polyclonal anti-mouse IL-18 antibody (1:100; Santa Cruz Biotechnology, Santa Cruz, CA (sc-6179) overnight at 4 °C) or a monoclonal anti-α-SMA antibody (1:1000, 1A4 clone, DakoCytomation, Carpinteria, CA, USA for 10 min). The slides were washed in TBS and incubated with the biotinylated secondary antibody (rabbit anti-goat, 1:100 for 1 h) or LSAB2 Kit (1:500, DakoCytomation) for 10 min. Peroxidase-stained sections were then developed with 3,3"-diaminobenzidine (DAB) or Streptavidin-HRP, and for IL-18, counterstained with hemalum for 30 s. Negative controls were performed without the primary antibody using idiotype-specific normal goat IgG. The extent of α-SMA staining in the renal cortex and medulla was semiquantitatively scored on a scale of 0–3, with 1 representing 5 to 15%, 2 representing 15 to 30%, and 3 representing >30% specific staining of the total kidney slice surface.

Masson's trichrome staining

Tissue sections were deparaffinized and rehydrated with alcohol. The slides were then washed in distilled water and stained in Weigert's iron hematoxylin working solution for 10 min. The slides were washed and stained in Biebrich scarlet-acid fuchsin solution for 15 min. The slides were then rewashed and differentiated in phosphomolybdic-phosphotungstic acid solution for 15 min. The tissue sections were then transferred directly to aniline blue solution for 5–10 min, rinsed, and differentiated in 1% acetic acid solution for 2–5 min. The slides were dehydrated, cleared in xylene, and mounted. The extent of staining in the renal cortex and medulla was semiquantitatively scored on a scale of 0–3, with 1 representing 5 to 15%, 2 representing 15 to 30%, and 3 representing >30% specific staining of the total kidney slice surface.

Western blot analysis

Protein extracts from homogenized samples (50 μg per lane) were subjected to SDS-PAGE electrophoresis on a Tris-Glycine gel and transferred to a nitrocellulose membrane. Immunoblotting was performed for each antibody by incubating each membrane in 5% dry milk overnight at 4 °C, followed by incubation with an anti-α-smooth muscle actin (α-SMA) monoclonal antibody (clone 1A4, 1:500 for 2 h at room temperature (RT), Sigma, St. Louis, MO, USA), an anti-E-cadherin monoclonal antibody (1:200 overnight at 4 °C, BD Transduction Laboratories, San Jose, CA, USA), or anti-RhoA monoclonal antibody (1:2000 for 2 h at RT, Santa Cruz Biotechnology, Santa Cruz, CA, USA). After washing three times in TBST, each membrane was incubated for 1 h at RT with a peroxidase-conjugated secondary antibody (1:2000 for α-SMA, 1:1000 for E-cadherin, and 1:10,000 for RhoA). Equivalent protein loading in each lane was confirmed by stripping and re-blotting each membrane for GAPDH (1:20,000 for 30 min at RT, secondary 1:20,000 for 30 min at RT; Biodesign International, Saco, ME, USA). The membranes were developed using enhanced chemiluminescence (Amersham Pharmacia Biotech Inc., Piscataway, NJ, USA), and the density of each band determined using NIH image analysis software and expressed as a percentage of GAPDH density.

Fibroblast and macrophage accumulation

Renal tissue sections were analyzed for the presence of transformed fibroblasts (EMT) utilizing an S100-A4 antibody (The S100-A4 antigen is also known as FSP-1)[8,57,58] and macrophage infiltration was determined with a rat anti-mouse macrophage antibody. Transverse 4 μm renal tissue sections were deparaffinized and dehydrated with xylene and alcohol. Antigen was retrieved by incubating the cells with proteinase K for 20 min in an oven. The tissues were then blocked with 1% bovine serum albumin (BSA) and incubated with a polyclonal rabbit antibody directed against S100-A4 (FSP-1; 1:200, DakoCytomation) for 1 h at 37 °C or the rat anti-mouse macrophage antibody (1:100, Angio-Proteomie, Boston, MA, USA) for 90 min at room temperature. Sections were washed and incubated with a secondary antibody (goat anti-rabbit (1:50)) or goat anti-rat (1:100) and incubated for 30 min. Peroxidase-stained sections were then developed with 3,3′′-diaminobenzidine and counterstained with hematoxylin (Sigma-Aldrich, St Louis, MO). Sections incubated without primary antibody exhibited no staining. Spindle-shaped FSP-1-positive cells and macrophage were counted in 10 high-powered fields (×400) in a blinded fashion and averaged.

Statistical analysis

Data are presented as mean values ± s.e.m. Differences at the 95% confidence level were considered significant. The experiment groups were compared using one-way ANOVA with *post hoc* Bonferroni-Dunn (JMP 5.0.1). For cell culture experiments using varying concentrations of IL-18, a multiple-comparison analysis was performed in all pairs using Tukey–Kramer HSD.

DISCLOSURE

All the authors declared no competing interests.

ACKNOWLEDGMENTS

This research was supported by NIH Grants DK065892 (KK Meldrum) and GM-070628 (DR Meldrum).

REFERENCES

1. Seikaly MG, Ho PL, Emmett L *et al.* Chronic renal insufficiency in children: the 2001 Annual Report of the NAPRTCS. *Pediatr Nephrol* 2003; **18**: 796–804.
2. Misseri R, Rink RC, Meldrum DR *et al.* Inflammatory mediators and growth factors in obstructive renal injury. *J Surg Res* 2004; **119**: 149–159.
3. Eddy AA. Molecular insights into renal interstitial fibrosis. *J Am Soc Nephrol* 1996; **7**: 2495–2508.
4. Klahr S. Progression of chronic renal disease. *Heart Dis* 2001; **3**: 205–209.

5. Remuzzi G, Bertani T. Pathophysiology of progressive nephropathies. *N Engl J Med* 1998; **339**: 1448–1456.
6. Healy E, Brady HR. Role of tubule epithelial cells in the pathogenesis of tubulointerstitial fibrosis induced by glomerular disease. *Curr Opin Nephrol Hypertens* 1998; **7**: 525–530.
7. Strutz F, Muller GA, Neilson EG. Transdifferentiation: a new angle on renal fibrosis. *Exp Nephrol* 1996; **4**: 267–270.
8. Strutz F, Okada H, Lo CW *et al.* Identification and characterization of a fibroblast marker: FSP1. *J Cell Biol* 1995; **130**: 393–405.
9. Zeisberg M, Bonner G, Maeshima Y *et al.* Renal fibrosis: collagen composition and assembly regulates epithelial-mesenchymal transdifferentiation. *Am J Pathol* 2001; **159**: 1313–1321.
10. Iwano M, Neilson EG. Mechanisms of tubulointerstitial fibrosis. *Curr Opin Nephrol Hypertens* 2004; **13**: 279–284.
11. Iwano M, Plieth D, Danoff TM *et al.* Evidence that fibroblasts derive from epithelium during tissue fibrosis. *J Clin Invest* 2002; **110**: 341–350.
12. Rastaldi MP. Epithelial-mesenchymal transition and its implications for the development of renal tubulointerstitial fibrosis. *J Nephrol* 2006; **19**: 407–412.
13. Rossini M, Cheunsuchon B, Donnert E *et al.* Immunolocalization of fibroblast growth factor-1 (FGF-1), its receptor (FGFR-1), and fibroblast-specific protein-1 (FSP-1) in inflammatory renal disease. *Kidney Int* 2005; **68**: 2621–2628.
14. Cheng S, Lovett DH. Gelatinase A (MMP-2) is necessary and sufficient for renal tubular cell epithelial-mesenchymal transformation. *Am J Pathol* 2003; **162**: 1937–1949.
15. Ikenouchi J, Matsuda M, Furuse M *et al.* Regulation of tight junctions during the epithelium-mesenchyme transition: direct repression of the gene expression of claudins/occludin by Snail. *J Cell Sci* 2003; **116**: 1959–1967.
16. Strutz F, Zeisberg M, Ziyadeh FN *et al.* Role of basic fibroblast growth factor-2 in epithelial-mesenchymal transformation. *Kidney Int* 2002; **61**: 1714–1728.
17. Xie L, Law BK, Chytil AM *et al.* Activation of the Erk pathway is required for TGF-beta1-induced EMT *in vitro*. *Neoplasia* 2004; **6**: 603–610.
18. Yang J, Liu Y. Dissection of key events in tubular epithelial to myofibroblast transition and its implications in renal interstitial fibrosis. *Am J Pathol* 2001; **159**: 1465–1475.
19. Zeisberg M, Hanai J, Sugimoto H *et al.* BMP-7 counteracts TGF-beta1-induced epithelial-to-mesenchymal transition and reverses chronic renal injury. *Nat Med* 2003; **9**: 964–968.
20. Ng YY, Huang TP, Yang WC *et al.* Tubular epithelial-myofibroblast transdifferentiation in progressive tubulointerstitial fibrosis in 5/6 nephrectomized rats. *Kidney Int* 1998; **54**: 864–876.
21. Li Y, Yang J, Dai C *et al.* Role for integrin-linked kinase in mediating tubular epithelial to mesenchymal transition and renal interstitial fibrogenesis. *J Clin Invest* 2003; **112**: 503–516.
22. Yang J, Liu Y. Blockage of tubular epithelial to myofibroblast transition by hepatocyte growth factor prevents renal interstitial fibrosis. *J Am Soc Nephrol* 2002; **13**: 96–107.
23. Bohn E, Sing A, Zumbihl R *et al.* IL-18 (IFN-gamma-inducing factor) regulates early cytokine production in, and promotes resolution of, bacterial infection in mice. *J Immunol* 1998; **160**: 299–307.
24. Daemen MA, van't Veer C, Wolfs TG *et al.* Ischemia/reperfusion-induced IFN-gamma up-regulation: involvement of IL-12 and IL-18. *J Immunol* 1999; **162**: 5506–5510.
25. Faust J, Menke J, Kriegsmann J *et al.* Correlation of renal tubular epithelial cell-derived interleukin-18 up-regulation with disease activity in MRL-Faslpr mice with autoimmune lupus nephritis. *Arthritis Rheum* 2002; **46**: 3083–3095.
26. Parikh CR, Jani A, Melnikov VY *et al.* Urinary interleukin-18 is a marker of human acute tubular necrosis. *Am J Kidney Dis* 2004; **43**: 405–414.
27. Rothe H, Jenkins NA, Copeland NG *et al.* Active stage of autoimmune diabetes is associated with the expression of a novel cytokine, IGIF, which is located near Idd2. *J Clin Invest* 1997; **99**: 469–474.
28. Striz I, Krasna E, Honsova E *et al.* Interleukin 18 (IL-18) upregulation in acute rejection of kidney allograft. *Immunol Lett* 2005; **99**: 30–35.
29. Parikh CR, Abraham E, Ancukiewicz M *et al.* Urine IL-18 is an early diagnostic marker for acute kidney injury and predicts mortality in the intensive care unit. *J Am Soc Nephrol* 2005; **16**: 3046–3052.
30. Dinarello CA, Novick D, Puren AJ *et al.* Overview of interleukin-18: more than an interferon-gamma inducing factor. *J Leukoc Biol* 1998; **63**: 658–664.
31. Netea MG, Fantuzzi G, Kullberg BJ *et al.* Neutralization of IL-18 reduces neutrophil tissue accumulation and protects mice against lethal Escherichia coli and Salmonella typhimurium endotoxemia. *J Immunol* 2000; **164**: 2644–2649.
32. Puren AJ, Fantuzzi G, Gu Y *et al.* Interleukin-18 (IFNgamma-inducing factor) induces IL-8 and IL-1beta via TNFalpha production from non-CD14+ human blood mononuclear cells. *J Clin Invest* 1998; **101**: 711–721.
33. Liang D, Liu HF, Yao CW *et al.* Effects of interleukin 18 on injury and activation of human proximal tubular epithelial cells. *Nephrology (Carlton)* 2007; **12**: 53–61.
34. Fantuzzi G, Banda NK, Guthridge C *et al.* Generation and characterization of mice transgenic for human IL-18-binding protein isoform a. *J Leukoc Biol* 2003; **74**: 889–896.
35. Chevalier RL. Obstructive nephropathy: towards biomarker discovery and gene therapy. *Nat Clin Pract Nephrol* 2006; **2**: 157–168.
36. Fan JM, Ng YY, Hill PA *et al.* Transforming growth factor-beta regulates tubular epithelial-myofibroblast transdifferentiation *in vitro*. *Kidney Int* 1999; **56**: 1455–1467.
37. Kuncio GS, Neilson EG, Haverty T. Mechanisms of tubulointerstitial fibrosis. *Kidney Int* 1991; **39**: 550–556.
38. Postlethwaite AE, Keski-Oja J, Moses HL *et al.* Stimulation of the chemotactic migration of human fibroblasts by transforming growth factor beta. *J Exp Med* 1987; **165**: 251–256.
39. Roberts AB, McCune BK, Sporn MB. TGF-beta: regulation of extracellular matrix. *Kidney Int* 1992; **41**: 557–559.
40. Alvarez RJ, Sun MJ, Haverty TP *et al.* Biosynthetic and proliferative characteristics of tubulointerstitial fibroblasts probed with paracrine cytokines. *Kidney Int* 1992; **41**: 14–23.
41. Border WA, Noble NA. Transforming growth factor beta in tissue fibrosis. *N Engl J Med* 1994; **331**: 1286–1292.
42. Humes HD, Cieslinski DA. Interaction between growth factors and retinoic acid in the induction of kidney tubulogenesis in tissue culture. *Exp Cell Res* 1992; **201**: 8–15.
43. Miyajima A, Chen J, Lawrence C *et al.* Antibody to transforming growth factor-beta ameliorates tubular apoptosis in unilateral ureteral obstruction. *Kidney Int* 2000; **58**: 2301–2313.
44. Chandrasekhar S, Harvey AK. Transforming growth factor-beta is a potent inhibitor of IL-1 induced protease activity and cartilage proteoglycan degradation. *Biochem Biophys Res Commun* 1988; **157**: 1352–1359.
45. Melnikov VY, Ecder T, Fantuzzi G *et al.* Impaired IL-18 processing protects caspase-1-deficient mice from ischemic acute renal failure. *J Clin Invest* 2001; **107**: 1145–1152.
46. Melnikov VY, Faubel S, Siegmund B *et al.* Neutrophil-independent mechanisms of caspase-1- and IL-18-mediated ischemic acute tubular necrosis in mice. *J Clin Invest* 2002; **110**: 1083–1091.
47. Du SH, Liu HF, Tang DS *et al.* [Expressions of IL-18Ralpha and IL-18Rbeta on rat primary renal tubular epithelial cells]. *Xi Bao Yu Fen Zi Mian Yi Xue Za Zhi* 2005; **21**: 293–295.
48. El-Obeid A, Bongcam-Rudloff E, Sorby M *et al.* Cell scattering and migration induced by autocrine transforming growth factor alpha in human glioma cells *in vitro*. *Cancer Res* 1997; **57**: 5598–5604.
49. Guo G, Morrissey J, McCracken R *et al.* Contributions of angiotensin II and tumor necrosis factor-alpha to the development of renal fibrosis. *Am J Physiol Renal Physiol* 2001; **280**: F777–F785.
50. Klahr S, Morrissey J. Angiotensin II and gene expression in the kidney. *Am J Kidney Dis* 1998; **31**: 171–176.
51. Haralambous-Gasser A, Chan D, Walker RG *et al.* Collagen studies in newborn rat kidneys with incomplete ureteric obstruction. *Kidney Int* 1993; **44**: 593–605.
52. Guo G, Morrissey J, McCracken R *et al.* Role of TNFR1 and TNFR2 receptors in tubulointerstitial fibrosis of obstructive nephropathy. *Am J Physiol* 1999; **277**: F766–F772.
53. Meldrum KK, Misseri R, Metcalfe P *et al.* TNF-alpha neutralization ameliorates obstruction-induced renal fibrosis and dysfunction. *Am J Physiol Regul Integr Comp Physiol* 2007; **292**: R1456–R1464.
54. Masszi A, Di Ciano C, Sirokmany G *et al.* Central role for Rho in TGF-beta1-induced alpha-smooth muscle actin expression during epithelial-mesenchymal transition. *Am J Physiol Renal Physiol* 2003; **284**: F911–F924.
55. Olee T, Hashimoto S, Quach J *et al.* IL-18 is produced by articular chondrocytes and induces proinflammatory and catabolic responses. *J Immunol* 1999; **162**: 1096–1100.
56. Kaneto H, Morrissey J, McCracken R *et al.* Enalapril reduces collagen type IV synthesis and expansion of the interstitium in the obstructed rat kidney. *Kidney Int* 1994; **45**: 1637–1647.
57. Barraclough R. Calcium-binding protein S100A4 in health and disease. *Biochim Biophys Acta* 1998; **1448**: 190–199.
58. El Chaar M, Chen J, Seshan SV *et al.* Effect of combination therapy with enalapril and the TGF-beta antagonist 1D11 in unilateral ureteral obstruction. *Am J Physiol Renal Physiol* 2007; **292**: F1291–F1301.